RSC Advances

PAPER

View Article Online
View Journal | View Issue

Anchoring effect on (tetra)carboxyphenyl porphyrin/TiO_2 composite films for VOC optical detection†‡

Cite this: *RSC Adv.*, 2014, **4**, 1974

Javier Roales,*[a] José M. Pedrosa,*[a] Manuel Cano,[a] María G. Guillén,[a] Tânia Lopes-Costa,[a] Pedro Castillero,[ab] Angel Barranco[b] and Agustín R. González-Elipe[b]

Received 16th May 2013
Accepted 6th November 2013

DOI: 10.1039/c3ra42443j

www.rsc.org/advances

The optical gas sensing properties of Zn-(II)-5,10,15,20-tetra(3-carboxyphenyl)porphyrin (*m*-ZnTCPP) and Zn-(II)-5,10,15,20-tetra(4-carboxyphenyl)porphyrin (*p*-ZnTCPP) bound to microcolumnar TiO_2 thin films have been compared and explained in terms of their different molecular structure and anchoring to the titania surface. This different binding has been confirmed by specular reflectance FTIR revealing that *m*-ZnTCPP is bound by its four carboxylic groups in contrast to *p*-ZnTCPP where two or three of these groups remain unanchored. As a consequence, the Soret band of the *para* derivative is blue shifted with respect to the solution, indicating H aggregation, while *m*-ZnTCPP remained in its monomeric form due to the planar anchoring by the four COOH groups to the titania matrix that would avoid porphyrin aggregation. The sensing performance of the two systems has been assessed by analyzing the spectral changes in their UV-visible spectra under exposure to six volatile organic compounds. Although the highly porous and non-dispersive TiO_2 matrix allow good sensing ability in both cases, the response of the *m*-ZnTCPP/TiO_2 composite has been found to be more intense and faster than that of *p*-ZnTCPP. Moreover, the use of identification patterns also indicates that the *meta* derivative achieves a more selective recognition of the selected analytes. This improvement in the sensing capabilities of *m*-ZnTCPP has been attributed to the absence of aggregation between adjacent macrocycles.

Introduction

Detection of volatile organic compound (VOC) has been generally performed through the separation and identification of components using gas chromatography or similar techniques. These analyses, although accurate, are usually time-consuming and need a lot of post-processing.[1] Alternatively, electronic nose technologies have been used to detect several kinds of compounds by an array of different sensors, providing an instantaneous and holistic response to the particular gas.[2,3] These devices are generally based on metal–oxide semiconductors and on conducting polymers.[4] They are appropriate for the discrimination of analytes of different chemical functionality, but not when these are within the same chemical class,[5] or when we try to detect metal-binding species.[6]

Porphyrins and other dyes have been widely used in the last decades for gas-sensitive purposes.[5,7–9] Their photochemical and photophysical properties make them ideal candidates for the optical detection of analytes. Thus, they can be precisely tuned by introducing substituents in their structure or coordinating metals to the porphyrin core.[8] However, one of the most challenging points of the development of a sensor based on porphyrins is the deposition onto solid substrates. Techniques such as Langmuir–Blodgett (LB), spin-coating or casting can be used to obtain solid films of the dyes, but the organization of these films in terms of molecular aggregation is sometimes unsatisfying, mainly because of the strong π–π interaction between porphyrins, which can strongly prevent a proper response to the analytes.[10] Several methods have been studied in order to avoid aggregation. In LB films, the addition of host molecules such as calixarenes has been found to reduce aggregates and hence improve the sensing properties of the films.[11,12] Spin coating and casting techniques may involve the use of polymers or other kind of molecules when the interaction between the substrate and the deposited material is weak, creating a host structure that improves the properties of the film and in some cases partially avoids porphyrin aggregation. Although the films made with these techniques can be improved using host molecules, there are other drawbacks. Despite the fact that LB films can be made under a high control

[a]*Departamento de Sistemas Físicos, Químicos y Naturales, Universidad Pablo de Olavide, Ctra. Utrera Km. 1, 41013 Sevilla, Spain. E-mail: jroabat@upo.es; jmpedpoy@upo.es*

[b]*Instituto de Ciencia de Materiales de Sevilla, Universidad de Sevilla – CSIC, Américo Vespucio 49, 41092, Sevilla, Spain*

† In memoriam of Tim H. Richardson.

‡ Electronic supplementary information (ESI) available. See DOI: 10.1039/c3ra42443j

of the quantity and orientation of molecules, the technique is time-consuming and the controlled structure does not always result in a substantial improvement of the sensing capabilities of the film. On the other hand, spin-coating and casting are straightforward techniques useful for the fast fabrication of porphyrin films, but the control over the structure and the amount of sensing material in the film may be minimal, especially in the case of casting.

Originally developed by solar cell researchers, the use of carboxylic acid derivatized molecules and their ability to chemically bind to TiO_2 allows the easy fabrication of stable composite films.[13] However, TiO_2 films prepared for solar cell purposes are usually thick and very dispersive, and thus inappropriate for gas sensing when using UV-visible spectroscopy. Microstructured TiO_2 films prepared by glancing angle physical vapor deposition (GAPVD) provide the perfect substrate for these composite films, given their transparency, high porosity, low refractive index and controlled thickness.[14] Films prepared by this technique have been used previously for gas sensing purposes and have been found to enhance the sensing properties of the porphyrins due to their open pores that facilitate the access to incoming gaseous molecules.[15–17] Also, the conformation of the sensing molecule in these composites can be important, determining its chemical binding to the substrate, according to the spatial distribution of anchoring points, and may also influence its tendency to aggregate with other molecules.[18] A change in the position of the peripheral substituents in a porphyrin can lead to different aggregation status that may improve its sensing capabilities.[10]

In a previous work,[17] we reported the gas-sensitive properties of 5,10,15,20-tetrakis(4-carboxyphenyl)-21*H*,23*H*-porphyrin and 10 of its metal derivatives, using microstructured columnar TiO_2 thin films prepared by GAPVD as host materials. The study of the chemical binding between these *para*-substituted tetracarboxyphenyl porphyrins and titania revealed that the dye molecules were likely to be bound by only one or two of their four available carboxylic acid groups, leading to a specific anchoring with the porphyrin rings lying perpendicular with respect to the TiO_2 surface which allowed face to face interaction. The gas sensing capabilities of the composite porphyrin/TiO_2 thin films showed fast, selective and concentration-dependent responses to the analyzed VOCs. However, it is known that the lack of aggregation enhances the sensing properties of porphyrins, allowing the gas molecules a better access to their coordination sites.[10] Therefore, the sensing system based on composite porphyrin/TiO_2 thin films may be improved by avoiding dye aggregation.

On the other hand, *para* and *meta* substituted tetraphenyl porphyrins are known to exhibit a different molecular structure.[18,19] While the substituents in the *para* position of the phenyl groups are situated in the plane of the molecule, the *meta* substituents are placed in a perpendicular direction with respect to the porphyrin ring. Based on this different molecular architecture, it has been demonstrated that *para* tetracarboxyphenyl porphyrins only anchor to the TiO_2 by one or two of the four carboxylic groups lying perpendicular to the metal oxide surface, while the *meta* derivatives can bind its four COOH groups lying parallel to the TiO_2 surface.[18] Our hypothesis is that these different arrangements can lead to a different aggregation status of the porphyrin that may influence its sensing capabilities, either in terms of response magnitude or kinetics.

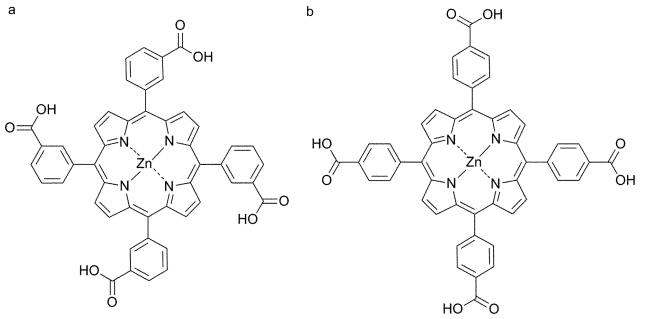

Fig. 1 Molecular structures of (a) Zn(II)-5,10,15,20-tetra(3-carboxyphenyl)porphyrin and (b) Zn(II)-5,10,15,20-tetra(4-carboxyphenyl) porphyrin.

In this work, we studied composite films made of microstructured columnar TiO_2 and, respectively, Zn-(II)-5,10,15,20-tetra(3-carboxyphenyl)porphyrin (*m*-ZnTCPP, Fig. 1a) and Zn-(II)-5,10,15,20-tetra(4-carboxyphenyl)porphyrin (*p*-ZnTCPP, Fig. 1b), and their sensing properties regarding both the anchoring to the TiO_2 and the molecule aggregation are compared. For this purpose, the chemical binding between the porphyrin and the TiO_2 has been confirmed through infrared spectroscopy. Besides, the influence of this binding on the aggregation and orientation of porphyrin molecules has been investigated. The optical responses of the two porphyrins to a total of 6 individual VOCs have been analyzed to test if the different peripheral substituent position plays an important role on the gas-sensing properties of these molecules.

Material and methods

Porphyrins and reagents

All porphyrins were purchased from Frontier Scientific, Inc. and used without further purification. All reagents were purchased from Sigma-Aldrich and used as received without further purification.

Film preparation

We prepared transparent and amorphous TiO_2 columnar films by the GAPVD technique at an angle of deposition of 70° with respect to the evaporation source. The angle formed by the columns and the substrate was approximately 60°, with a film thickness of approximately 350 nm exhibiting an elevated porosity (total pore volume of 49%) with void apertures on the surface in the form of mesopores (pore diameter >2 nm), that also determines a relatively low refractive index value, that was found to be 1.79.[15] Further details regarding film preparation, SEM images and structural information can be found elsewhere.[17] The high porosity of the films would allow the accessibility of both porphyrins during the composite film preparation

and VOCs during the gas sensing experiments. For specular reflectance Fourier transform infrared (FT-IR) spectroscopy, the films were deposited on gold-coated silicon substrates. Films for UV-visible spectroscopy were prepared on glass substrates. Binding of porphyrins to the TiO_2 films was performed by immersion of the substrates in a 10^{-4} M MeOH solution of the dye for 1 h. After this, the films were rinsed with MeOH to remove physisorbed dye molecules and dried in air. Prior to the measurements, all films were heated to 110 °C for 30 min to desorb any contaminant and allowed to cool to room temperature (21 °C) under a dry N_2 stream.

Infrared and UV-visible spectroscopy

We performed the study of the binding of the carboxylic porphyrins to TiO_2 through specular reflectance FT-IR spectroscopy using a Jasco FT/IR-6200 spectrometer. The specular reflectance FT-IR spectra for the porphyrins were measured neat (by casting on silicon substrates) and bound to the TiO_2 thin films. All spectra were obtained using typically 500 scans with a resolution of 4 cm^{-1}. To remove the background, we subtracted the signal obtained from a gold substrate.

UV-visible spectra of the porphyrins were recorded in MeOH solution using an Ocean Optics USB4000 spectrophotometer.

Gas exposure

We used a gas testing chamber connected through optical fibers to a World Precision Instruments SpectroMate spectrophotometer to expose the samples to the VOCs and register their UV-vis spectrum simultaneously. The chamber consisted of a gas inlet and an outlet, a Peltier heating–cooling device and housings for the two optical fibers that deliver and collect the light for the optical measurements. Further details regarding this setup can be found elsewhere.[20] We obtained the gaseous VOCs by bubbling dry nitrogen through a bottle containing the desired liquid VOC immersed in a temperature-controlled water bath. The resulting gas was composed by dry nitrogen saturated in each VOC, whose concentration can be calculated through its vapor pressure at the corresponding temperature. Vapor pressures were controlled by regulating the bath temperature, 20 °C in all cases except for the VOC concentration dependence experiments where a temperature of 0 °C was used in order to avoid a possible condensation of the analyte inside the gas chamber or the tubing system. In order to obtain the exact desired concentration, we diluted the VOC–N_2 gas stream with another N_2 gas stream, and calculated the final concentration by applying the dilution factor. Analogous procedures for the generation of low concentrations of VOCs can be found in the literature.[6]

Immediately before the gas exposure phase, we introduced dry N_2 in the gas chamber to desorb completely any possible contaminating gases from the inner walls and hence preventing the contamination of the samples. Then, we inserted the samples into the gas chamber and again dry N_2 was introduced into the chamber to allow complete desorption of possible contaminating gases adsorbed on the sample. After this, we directed the gas mixture (VOC and N_2) into the gas chamber until complete saturation of the porphyrin, typically a few seconds as detailed elsewhere.[17] We exposed all samples to the gases at room temperature (~293 K). For the recovery phase, we introduced dry N_2 again while heating the samples at relatively high temperature (~383 K) to remove all the VOC gases from the chamber and the samples.

Data analysis

The study of differences between before and after exposure spectra was accomplished by the analysis of the absolute value of the difference spectrum, obtained in each case by subtracting the non-exposure spectrum to the exposure one and calculating the absolute values of the absorbance corresponding to each wavelength.

In order to compare easily the different responses of the porphyrins to the analytes, we created identification patterns for each case, resulting in an image which shows the behavior of each of the porphyrins to the VOCs vapors. For each porphyrin and analyte, we subtracted the non-exposure spectrum from the exposure one at each wavelength and normalized to the maximum absorbance of the non-exposed spectrum. All the difference spectra in absolute value for each porphyrin in the Soret band region were converted into an $m \times n$ matrix (where m is the wavelength and n is the number of analytes, $n = 6$ in this case) which was represented as color image using Origin Pro 8 software. Through this representation, a barcode like image consisting of 6 columns and m rows, in which the different values ($m \times 6$ pixels) are colored from red to blue (*i.e.*, non change points are represented in red and maximum change points are colored in blue), was created for each porphyrin.

Results and discussion

Binding to TiO_2

Specular reflectance FT-IR spectra of *meta* and *para* porphyrins neat and bound to TiO_2 are shown in Fig. 2. In all cases, the existence of typical bands corresponding to the symmetric and asymmetric stretching modes of the pyrrole ring (ν (C–H), ν (C=C) and ν (C=N)) within the *meso*-tetraphenylporphyrin macrocycle was evident over the range 700–1500 cm^{-1}.[21] The binding interaction between the TCPP and the metal oxide surface is revealed by the comparison of changes in the region of the carbonyl group in the FT-IR spectra. Neat samples of *m*-ZnTCPP showed two strong bands at 1732 cm^{-1} and 1294 cm^{-1} which are characteristic of the ν (C=O) stretch and the ν (C–O) stretch of the carboxylic acid groups, respectively. In the case of *p*-ZnTCPP, where the –COOH groups are situated in the plane of the tetrapyrrole macrocycle, the extensive hydrogen bonding of the carboxylic acid groups resulted in a shift to lower frequency of the ν (C=O) stretch at 1690 cm^{-1} and a shift to higher frequency of the ν (C–O) stretch at 1402 cm^{-1}.[22]

Upon binding of *m*-ZnTCPP to TiO_2, the ν (C=O) and ν (C–O) stretching modes disappeared completely, and new bands appeared in the 1385–1440 cm^{-1} and 1530–1570 cm^{-1} regions, corresponding to the symmetric and asymmetric ν (CO_2^-) stretches, respectively. In the case of *p*-ZnTCPP/TiO_2, the bands

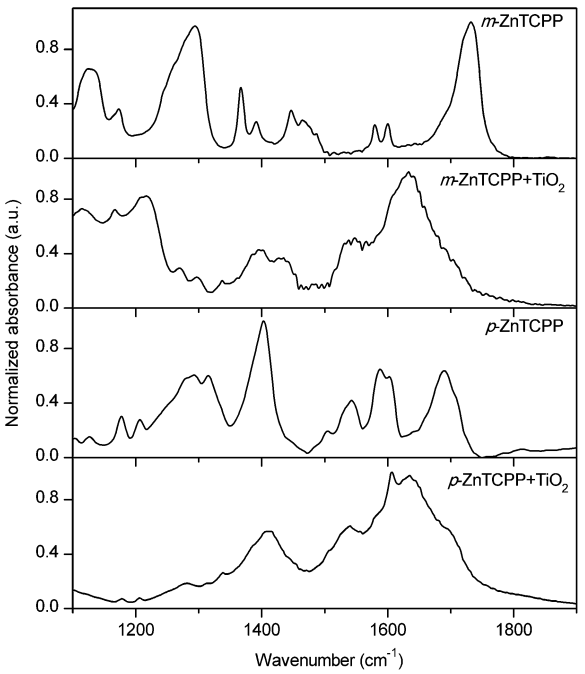

Fig. 2 Specular reflectance FT-IR spectra of *m*-ZnTCPP and *p*-ZnTCPP neat (by casting on silicon substrates) and bound to TiO_2.

corresponding to the C═O and C–O stretching modes were still partially present with a slight broadening of the latter. In this case, the appearance of the band corresponding to the symmetric ν (CO_2^-) stretch is not so evident due to overlapping with the remaining ν (C–O) stretch band. Moreover, the changes in the 1500–1750 cm^{-1} region, where the asymmetric ν (CO_2^-) stretch band was expected to appear, were hindered by the presence of a strong and broad band around 1630 cm^{-1} corresponding to the free TiO_2 molecules of the columnar film (Fig. S1 in the ESI‡).

Chemical binding of carboxylic acids to TiO_2 colloidal films has been associated with the disappearance of the bands corresponding to the ν (C═O) and ν (C–O) stretching modes, and the appearance of strong and broad bands at ~1400 cm^{-1} and ~1550 cm^{-1}, characteristic of the symmetric and asymmetric ν (CO_2^-) stretches respectively.[18] These spectral changes have been found to be compatible with chelating and/or bidentate binding modes of the carboxylate groups on the TiO_2 surface.[18,23–26]

The IR spectrum of *m*-ZnTCPP/TiO_2 was consistent with the absence of free carboxylic acid groups, given that C═O and C–O stretching modes disappeared completely. This suggests a planar situation of the porphyrin macrocycle with respect to the titania surface in which all carboxyl groups are bound to the TiO_2.[18] However, in the case of *p*-ZnTCPP/TiO_2, the stretching modes corresponding to C═O and C–O disappeared only partially, indicating the presence of free carboxylic acid groups coexisting with carboxylate groups bound to TiO_2. As a result of this, and due to the planar structure of the *para* substituted pophyrins, it can be expected that they are bound only by one or two of its four carboxyl groups to the metal oxide surface, resulting in a perpendicular orientation of the molecule with respect to the surface that allows them to interact (face to face) with other molecules, causing aggregation.[18,27]

Aggregation of dye molecules

In the UV-visible solution spectra, both *m*-ZnTCPP and *p*-ZnTCPP appeared in their monomeric form with the Soret band centered at 423 nm (Fig. 3). When bound to the TiO_2, *m*-ZnTCPP showed a slight broadening of the Soret band (Fig. 3a), although its peak remained at 423 nm as the solution spectrum, indicating that the porphyrin was predominantly in its monomeric form. However, the spectrum of *p*-ZnTCPP in the film featured a broadening and blue shift (10 nm) of the Soret band with respect to the solution spectrum (Fig. 3b), which indicated that the dye molecules were arranged mostly as H-aggregates.[18,28,29] The broadening of the Soret band has been attributed to the coexistence of monomers alongside of H and J aggregates, where the main peak is centered at the wavelength of the predominant species.[30]

The results from the IR experiments support these assumptions. In the case of *m*-ZnTCPP, where all carboxylic groups are bound to the titania substrate, the macrocycle lies parallel to the surface avoiding contact between porphyrin rings and hence preventing aggregation. This is not the case of *p*-ZnTCPP, which is presumably bound to the TiO_2 matrix by only two of its four carboxylic groups, leaving the porphyrin ring normal to the surface and allowing π–π interactions between nearby molecules. With this arrangement, the formation of H or J aggregates is determined by the relative position of adjacent porphyrin molecules, according to the microstructure of the substrate where they are anchored.

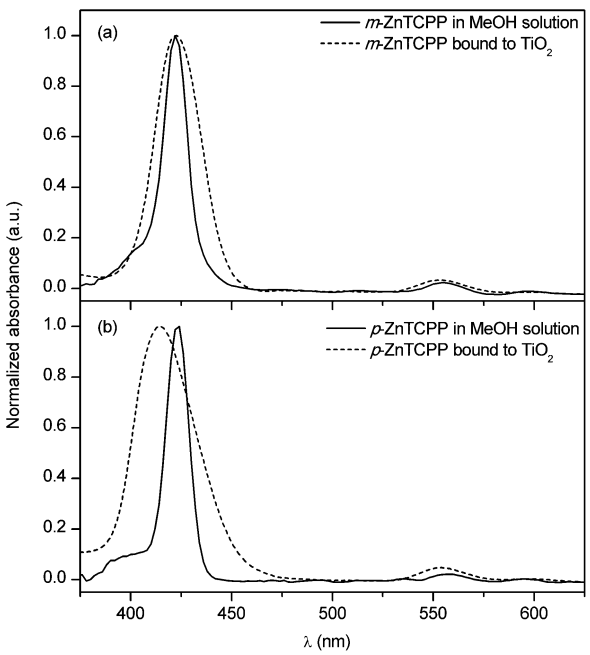

Fig. 3 UV-visible absorption spectra of (a) *m*-ZnTCPP and (b) *p*-ZnTCPP in methanol solution (solid line) and bound to TiO_2 film (dashed line).

Porphyrin aggregation may hamper the access of the gaseous analytes to the porphyrin coordination sites, and hence be unfavorable for gas sensing purposes.[10] Although the interaction between macrocycles might not be strong enough to impede analyte binding, the lack of aggregation is beneficial for gas sensing purposes because it allows porphyrin π systems to be completely available to incoming gaseous molecules.

Gas sensing

Composite porphyrin/TiO_2 films prepared with *m*-ZnTCPP and *p*-ZnTCPP were exposed to acetone, acetonitrile, butylamine, chloroform, ethanol and tetrahydrofuran. To study the differences in their sensing performance, the difference spectra of the composite films upon their exposure to acetone, acetonitrile and tetrahydrofuran, in absolute value, alongside with the non-exposed and exposed spectra, have been analyzed (Fig. 4). All samples featured important changes in their spectra during the exposure to the analytes, confirming the ability of porphyrins for the detection of VOCs. Specifically, metalloporphyrins are known for their ability to detect metal-ligating compounds because of their notable spectral changes upon ligand interaction and their open coordination sites for axial ligation.[7,31]

Focusing on the difference spectra, which allow a better comparison of the spectral changes among the cases studied here, *m*-ZnTCPP response was different when exposed to the three VOCs, whereas *p*-ZnTCPP spectral changes were more uniform in the three cases. It can be seen that the relative heights of the two peaks in the *m*-ZnTCPP difference spectra are different in each case, suggesting a more selective response to the analytes. In the acetone difference spectrum, the left peak is clearly higher than the right one, while in contrast, the behavior of the exposure to tetrahydrofuran is the opposite and the exposure to acetonitrile resulted in a difference spectrum with two peaks of approximately the same height. On the other hand, the changes exhibited by *p*-ZnTCPP after the exposure to the VOCs were very similar, being the relative heights and shapes of the peaks corresponding to the difference spectra almost identical. With this information, we can expect a better sensing performance from the *meta* substituted porphyrin in terms of selectivity.

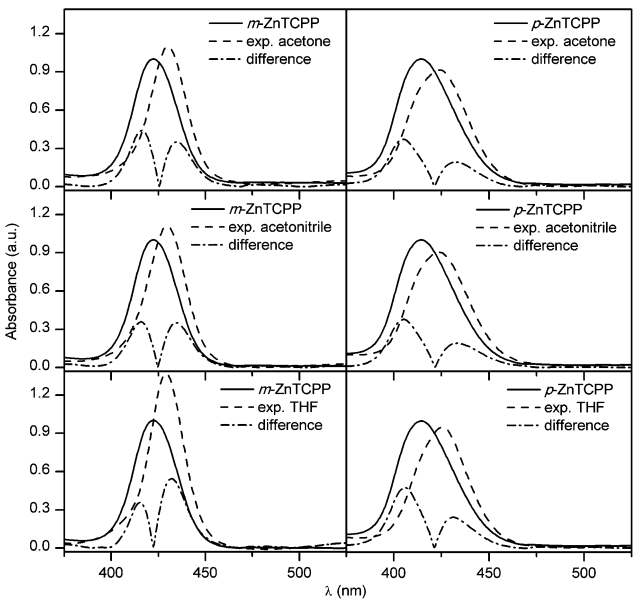

Fig. 4 Top: Pre-exposure (solid line), exposure (dashed line) and difference (dashed dotted line) spectra of *m*-ZnTCPP/TiO_2 (left) and *p*-ZnTCPP/TiO_2 (right) composite films upon exposure to acetone, acetonitrile and tetrahydrofuran.

Metal derivatives of *p*-TCPP have shown to be good candidates for the construction of selective optical sensors.[17] In this case, a large number of metal derivatives is needed to ensure a good selectivity through the use of recognition patterns. Such selectivity can be significantly improved by the use of *m*-TCPPs since their absorbance spectrum is not affected by aggregation, with a narrower Soret band in its monomeric form being able to exhibit more specific changes in the presence of the different analytes. Moreover, this lack of aggregation can also improve the sensor sensing ability through more pronounced spectral changes and its speed of response.

The spectral changes observed during the exposure of the composite films to all analytes are available in the ESI (Fig. S2‡). Upon exposure to the different compounds, all samples experienced significant changes in their respective spectra. All films returned to their initial status after the recovery procedure. Repeatability and reversibility of the system was confirmed through the cyclic exposure and recovery of the samples to the analytes, finding no differences between cycles.

In order to quantify the spectral response of the two porphyrins to all VOCs, we defined the change fraction as the area of the difference spectrum, obtained by subtracting the exposed spectrum to the unexposed one, divided by the area of the unexposed spectrum. The value that is obtained through this procedure gives an idea of the quantity of change that a porphyrin experiences, referred to its initial spectrum to make all responses comparable irrespective of the quantity of material deposited in the film. The change fraction for each case is shown in Fig. 5. In all cases, *m*-ZnTCPP showed a higher response than *p*-ZnTCPP, being the difference of at least 10%. This was especially relevant in the detection of butylamine, ethanol and tetrahydrofuran, where the *meta* substituted porphyrin yielded a response between 50 and 95% higher than *p*-ZnTCPP, according to their change fraction. Similar representations that summarize the spectral changes of porphyrins for gas-sensing purposes can be found in the literature.[32] As was observed in Fig. 4, both porphyrins showed good sensing capabilities to the selected compounds. This is confirmed by the change fraction values, which ranged from 0.2 to 1, showing that in all cases the spectra changed appreciably. However, it is noticeable that *m*-ZnTCPP featured a higher response to the analytes than *p*-ZnTCPP, indicating that aggregation between porphyrin molecules may be detrimental for gas sensing purposes.

The quantification of the spectral change provided us an easy way of comparing the gas sensing properties of the two analyzed porphyrins, but in this process some of the information contained in the spectra, such as the shape of the peaks or

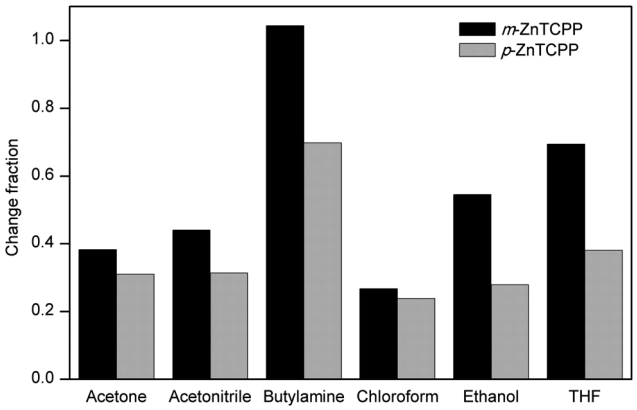

Fig. 5 Change fraction values corresponding to the exposure of *m*-ZnTCPP/TiO_2 (black) and *p*-ZnTCPP/TiO_2 (gray) composite films to acetone, acetonitrile, butylamine, chloroform, ethanol and tetrahydrofuran.

the wavelengths where they are located is necessarily discarded. By the creation of identification patterns we incorporated all the information provided by the spectra into a single image that depicts graphically the behavior of the sensing system (Fig. 6). A similar procedure has been used previously to create fingerprints for several VOCs based on the changes that they induced to the sensing material.[17] At a glance, it can be noticed that the patterns in *m*-ZnTCPP showed more variations among analytes than in the case of *p*-ZnTCPP. A more in-depth analysis of the images reveals that all bands corresponding to the different analytes in *m*-ZnTCPP showed appreciable differences among them, either in intensity or in position, which can be translated into a better selectivity of the system. On the contrary, *p*-ZnTCPP identification patterns were clearly more uniform. In particular, the patterns corresponding to acetone, acetonitrile and tetrahydrofuran are almost identical. In this case, the discrimination

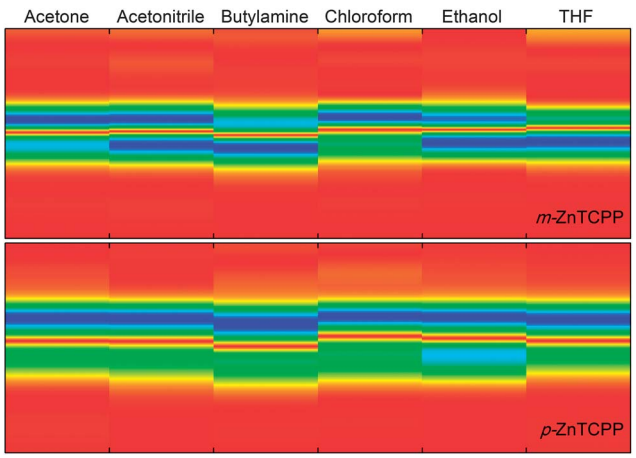

Fig. 6 Identification patterns obtained for acetone, acetonitrile, butylamine, chloroform, ethanol and tetrahydrofuran corresponding to *m*-ZnTCPP/TiO_2 and *p*-ZnTCPP. Color scale goes from red to blue, where red means no change between exposed and non-exposed spectra and blue is the highest change detected.

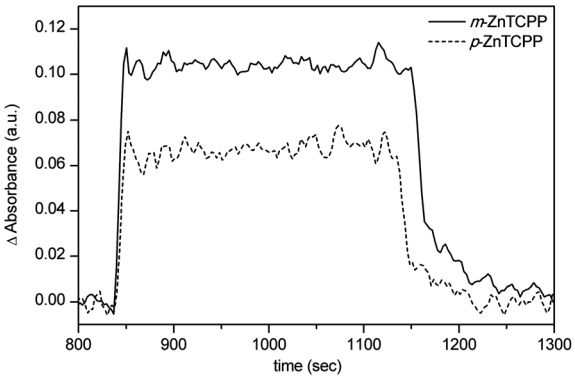

Fig. 7 Kinetics of the exposure of *m*-ZnTCPP (433 nm) and *p*-ZnTCPP (431 nm) composite films to 100 ppm EtOH vapor.

of these analytes using only the spectral information provided by the *para* substituted porphyrin would be difficult.

Sensor kinetics

To assess the influence of the peripheral substituents on the porphyrin performance, the kinetics of *m*-ZnTCPP/TiO_2 and *p*-ZnTCPP/TiO_2 films was studied. For this purpose, the composite films were exposed to 100 ppm EtOH and their absorbance at the wavelength of maximum change was recorded through time (Fig. 7). The exposure of the porphyrins to EtOH resulted in an increment of the absorbance at the measured wavelength (433 nm for *m*-ZnTCPP and 431 nm for *p*-ZnTCPP) as a result of the interaction with the analyte. The spectra of both porphyrins returned to their original status during the recovery phase. To provide a quantification for the different kinetics in each case, the value of t_{50}, which is the time taken for the absorbance to reach the 50% of its total maximum change, was calculated. Mean t_{50} after three cycles of exposure-recovery was 1.56 s in case of *m*-ZnTCPP, and 3.2 s for *p*-ZnTCPP. The fast responses can be attributed to the high responsiveness of Zn porphyrins[17] and to the TiO_2 porous matrix, which allows a fast diffusion of gases through its internal structure, making them instantly available to the dye molecules.[14] However, regarding the comparison of our two systems, *m*-ZnTCPP kinetics was twice as fast as *p*-ZnTCPP. The differences in the speed of response, altogether with the results from the change fraction comparison and the identification patterns analysis, show that *m*-ZnTCPP/TiO_2 films exhibited better gas-sensing properties than those based on *p*-ZnTCPP. This confirms that the positioning of the carboxylic acids in *meta* position in the porphyrins studied here improves considerably the sensing capabilities of the porphyrin/TiO_2 system. Therefore, our hypothesis that a change in the position of the peripheral substituents in a porphyrin can lead to different aggregation status that may improve its sensing capabilities, either in terms of response magnitude or kinetics can be validated.

Conclusions

Composite porphyrin/TiO_2 films based on microstructured columnar TiO_2 as host material and either *para* or *meta*-substituted

Zn tetracarboxyphenyl porphyrins as sensing molecules have been prepared. Specular reflectance FT-IR has confirmed that the chemical binding of the two porphyrins to the TiO_2 is different depending on the corresponding position of the carboxylic acid groups. In particular, the dye molecules with the COOH groups in *meta* position were bound by their four carboxylic groups, whereas two or three of these groups remained unanchored in the *para* derivative. When hosted in the film, *p*-ZnTCPP featured a broadening and blue shift of the Soret band with respect to the solution spectrum, which indicated that the dye molecules were arranged mostly as H-aggregates. In contrast, the spectrum of *m*-ZnTCPP remained in its monomeric form, which has been attributed to the planar anchoring by the four carboxylic groups to the titania matrix that would prevent porphyrin aggregation.

The gas-sensitive properties of the *m*-ZnTCPP and *p*-ZnTCPP/TiO_2 composites have been studied by analyzing the spectral changes undergone by the porphyrins in the UV-visible region upon their exposure to six different VOCs. All samples featured important changes in their spectra during the exposure to the analytes, confirming the abilities of these systems for the detection of VOCs. However, the response magnitude, quantified through the creation of the change fraction parameter, was considerably higher for *m*-ZnTCPP as compared to *p*-ZnTCPP. Furthermore, the use of identification patterns based on spectral images clearly shows that the *meta* derivative offers a more selective response to the different analytes, paving the way for the preparation of multisensor arrays based on metal derivatives of *m*-TCPP with enhanced selectivity towards isolated and mixed analytes. Finally, the kinetics of the exposure has also revealed that the *m*-ZnTCPP response was twice as fast as *p*-ZnTCPP.

Overall, the *m*-ZnTCPP/TiO_2 films exhibited better gas-sensing properties than those based on *p*-ZnTCPP as a consequence of the different position of the peripheral carboxylic groups, whose specific anchoring to the titania surface leads to a different aggregation state in the solid film.

Acknowledgements

We thank the Ministerio de Economía y Competitividad of Spain (Project TEC2010-21830-C02-01) for financial support.

References

1 H. T. Nagle, S. S. Schiffman and R. Gutierrez-Osuna, *IEEE Spectrum*, 1998, **35**, 22–34.
2 J. W. Gardner and B. N. Bartlett, *Electronic Noses: Principles and Applications*, Oxford University Press, New York, 1999.
3 F. Röck, N. Barsan and U. Weimar, *Chem. Rev.*, 2008, **108**, 705–725.
4 K. J. Albert, N. S. Lewis, C. L. Schauer, G. A. Sotzing, S. E. Stitzel, T. P. Vaid and D. R. Walt, *Chem. Rev.*, 2000, **100**, 2595–2626.
5 N. A. Rakow, A. Sen, M. C. Janzen, J. B. Ponder and K. S. Suslick, *Angew. Chem., Int. Ed.*, 2005, **44**, 4528–4532.
6 N. A. Rakow and K. S. Suslick, *Nature*, 2000, **406**, 710–713.
7 K. S. Suslick, D. P. Bailey, C. K. Ingison, M. Janzen, M. E. Kosal, W. B. McNamara, III, N. A. Rakow, A. Sen, J. J. Weaver, J. B. Wilson, C. Zhang and S. Nakagaki, *Quim. Nova*, 2007, **30**, 677–681.
8 C. Di Natale, R. Paolesse, A. D'Amico, C. Dinatale and A. Damico, *Sens. Actuators, B*, 2007, **121**, 238–246.
9 J. M. Pedrosa, C. M. Dooling, T. H. Richardson, R. K. Hyde, C. A. Hunter, M. T. Martín and L. Camacho, *Mater. Sci. Eng., C*, 2002, **22**, 433–438.
10 J. M. Pedrosa, C. M. Dooling, T. H. Richardson, R. K. Hyde, C. A. Hunter, M. T. Martín and L. Camacho, *Langmuir*, 2002, **18**, 7594–7601.
11 G. De Miguel, M. Martín-Romero, J. M. Pedrosa, E. Muñoz, M. Pérez-Morales, T. H. Richardson and L. Camacho, *J. Mater. Chem.*, 2007, **17**, 2914–2920.
12 J. Roales, J. M. Pedrosa, P. Castillero, M. Cano and T. H. Richardson, *Thin Solid Films*, 2011, **519**, 2025–2030.
13 W. M. Campbell, A. K. Burrell, D. L. Officer and K. W. Jolley, *Coord. Chem. Rev.*, 2004, **248**, 1363–1379.
14 J. R. Sánchez-Valencia, A. Borrás, A. Barranco, V. J. Rico, J. P. Espinós, A. R. González-Elipe, J. R. Sánchez-Valencia, A. Borrás, J. P. Espinos and A. R. González-Elipe, *Langmuir*, 2008, **24**, 9460–9469.
15 P. Castillero, J. R. Sánchez-Valencia, M. Cano, J. M. Pedrosa, J. Roales, A. Barranco and A. R. González-Elipe, *ACS Appl. Mater. Interfaces*, 2010, **2**, 712–721.
16 M. Cano, P. Castillero, J. Roales, J. M. Pedrosa, S. Brittle, T. Richardson, A. R. González-Elipe and A. Barranco, *Sens. Actuators, B*, 2010, **150**, 764–769.
17 J. Roales, J. M. Pedrosa, P. Castillero, M. Cano, T. H. Richardson, A. Barranco and A. R. González-Elipe, *ACS Appl. Mater. Interfaces*, 2012, **4**, 5147–5154.
18 J. Rochford, D. Chu, A. Hagfeldt and E. Galoppini, *J. Am.Chem. Soc.*, 2007, **129**, 4655–4665.
19 B. R. Takulapalli, G. M. Laws, P. a. Liddell, J. Andréasson, Z. Erno, D. Gust and T. J. Thornton, *J. Am. Chem. Soc.*, 2008, **130**, 2226–2233.
20 C. M. Dooling, O. Worsfold, T. H. Richardson, R. Tregonning, M. O. Vysotsky, C. A. Hunter, K. Kato, F. Kaneko and K. Shinbo, *J. Mater. Chem.*, 2001, **11**, 392–398.
21 B. Long, K. Nikitin and D. Fitzmaurice, *J. Am. Chem. Soc.*, 2003, **125**, 5152–5160.
22 E. Galoppini, J. Rochford, H. Chen, G. Saraf, Y. Lu, A. Hagfeldt and G. Boschloo, *J. Phys. Chem. B*, 2006, **110**, 16139–16161.
23 G. Deacon and R. Phillips, *Coord. Chem. Rev.*, 1980, **33**, 227–250.
24 K. S. Finnie, J. R. Bartlett and J. L. Woolfrey, *Langmuir*, 1998, **14**, 2741–2749.
25 A. Vittadini, A. Selloni, F. P. Rotzinger and M. Grätzel, *J. Phys. Chem. B*, 2000, **104**, 1300–1306.
26 M. K. Nazeeruddin, R. Humphry-Baker, P. Liska and M. Grätzel, *J. Phys. Chem. B*, 2003, **107**, 8981–8987.
27 J. Rochford and E. Galoppini, *Langmuir*, 2008, **24**, 5366–5374.
28 N. Aratani, A. Osuka, H. S. Cho and D. Kim, *J. Photochem. Photobiol., C*, 2002, **3**, 25–52.

29 M.-S. Choi, *Tetrahedron Lett.*, 2008, **49**, 7050–7053.
30 G. De Miguel, M. T. Martín-Romero, J. M. Pedrosa, E. Muñoz, M. Pérez-Morales, T. H. Richardson, L. Camacho, G. De Miguel and M. Martín-Romero, *Phys. Chem. Chem. Phys.*, 2008, **10**, 1569–1576.
31 K. S. Suslick, N. a. Rakow and A. Sen, *Tetrahedron*, 2004, **60**, 11133–11138.
32 A. D. F. Dunbar, T. H. Richardson, A. J. McNaughton, J. Hutchinson and C. A. Hunter, *J. Phys. Chem. B*, 2006, **110**, 16646–16651.